

The effect of interfacial mixing on Ag/Al₂O₃ by N⁺ implantation

TIAN JUN, XUE QUNJI

*Laboratory of Solid Lubrication, Lanzhou Institute of Chemical Physics,
Chinese Academy of Sciences, Lanzhou 730000*

E-mail: tianjun@public.lz.gs.cn

WANG QIZU

Department of Materials Science, Lanzhou University, Lanzhou 730000

CHEN YUFENG

China Building Materials Academy, Beijing 100024

The Ag film/Al₂O₃ implanted with an N ion energy of 110 keV. The ion-induced interfacial mixing were examined using AES, STD and XPS. The frictional coefficient of implanted Ag/Al₂O₃ in air was determined by Drive friction precise measuring apparatus (DFPM). The influence of N⁺ implantation on the interfacial chemistry and adhesion of Ag films on Al₂O₃ substrates was examined, compounds formed by introducing a thin layer between the Ag and the Al₂O₃ at $1 \times 10^{17} \text{ N} \cdot \text{cm}^{-2}$. This investigation resulted in extensive interfacial grading, and new chemical bonding across the Ag/Al₂O₃ interfaces. The case for the Ag/Al₂O₃ reaction lead to the metal ceramic of 13Al₂O₃ · AlN and α-AgAlO₂ formation though non equilibrium processes of implantation, and friction decreased in initial cycle where ion implantation of lower vacuum lead to surface carbon film. The combination of these effects provided an adhesion increase that was approximately 3 times that obtained in unimplanted Ag/Al₂O₃ specimens. © 1999 Kluwer Academic Publishers

1. Introduction

The previous work indicated that the friction coefficients and the wear rates of the most commonly used ceramics were unacceptably high under “dry” conditions. Effort has been devoted very recently to surface modifications for ceramics [1–4]. The importance of both self-lubrication and electrical conductive paths was predicted on metal/ceramics, one problem is the poor adhesion between metallic film and the oxide [5]. Excellent and permanent adhesion of the coatings to the substrate is essential for applications [6] such as, for example, contacts and friction in device packing or optical coatings. Ion beam mixing technology by irradiating inactive or active ion beam has been found to provide a versatile and powerful means of modifying the interface at the atomic scale [7]. These modification were attributed to microstructural changes caused by the implantation [8]. In many instances, films adhere poorly to substrates due to interfacial bond factors. The ion implantation technique can be able to break the atomic bonding terminated at the substrate surface or to mobilize atoms near the interface, which results in forming a complex chemical bonding structure linking the film and substrate. Ion beam mixing can be used to constructively alter many of these factors critical to good adhesion without modifying the bulk substrate properties [9, 10] and formed the new compound in non equilibrium processes which was not obtained by general

synthetic reaction. In fact, there is a strong correlation between the extent of the mixing and the thermochemical properties: the heat of mixing and the cohesive energy of the solids, a semi-empirical “enthalpy rule” can be formulated [11]. Enhanced mixing occurs whenever any of the possible chemical reaction between the film and the substrate has a negative reaction enthalpy. The influence of low temperature reactive ion beam mixing on interfacial chemistry and adhesion was examined for nickel films on glassy carbon substrates. The changes of interfaces by high energy implantation in Au or Ag/Al₂O₃ systems have been investigated at 300 K [12], with the formation of silver or gold metallic precipitates embedded into Al₂O₃. In this study, we are concerned with mechanisms for adhesion enhancement in the Ag/Al₂O₃ system by N ion beam mixing, change in the chemical bond producing the reactive adhesion promoters in lower vacuum.

2. Experimental

Single α-Al₂O₃ (ruby) crystal (1 0 4) surface, Al₂O₃ blocks were cut into $\phi 15 \text{ mm} \times 1.5 \text{ mm}$ samples. The specimen were ground to levels of assured planarity on rotating metallic discs using a diamond paste of 3 μm grain size (surface roughness <0.02 μm). To reduce damage induced by the polishing, the specimen were post-annealed in air for 15 h at 1200 °C. A high voltage

of 1.5 kV was applied to the system during the ion-plating process of Ag on the ceramic substrate. The thickness of the thin ion-plating Ag film on Al_2O_3 substrate was determined with an optical interference microscope. Then the thickness of a thin ion-plating Ag film on $\alpha\text{-Al}_2\text{O}_3$ was about $0.11 \pm 0.02 \mu\text{m}$ using optical interference microscope. The Ag film/ Al_2O_3 implanted with an N ion energy of 110 keV. The pressure of the target chamber was about 4–7 mPa during implantation. The ion dose of each specimen is 1×10^{15} , 1×10^{16} and $1 \times 10^{17} \text{ cm}^{-2}$. Parts of each sample were shielded from the ion bombardment to retain unimplanted areas to allow measurements on crystal surface with the same history. To avoid heating effects the samples were clamped onto a watercooled copper plate, and the ion current densities were kept 16–20 $\mu\text{A}/\text{cm}^2$.

The film adhesion enhancement was employed using a WS-91 automatic scratch tester. Scratch test was performed equipped with a 120° diamond indenter, the radius of used indenter vertex was 0.2 mm. The construction of the tester is almost similar to a pickup of the record player. The specimen is slowly moved to a direction, while the load of indenter is gradually increased. When the surface of the film is not broken, and the indenter only slides on the surface. When the load reaches a critical load, the surface of the film is broken, and output from pickup is observed as scratch noise. The adhesion between two materials depends on the morphological and chemical properties of the interface. In this work, load increasing from 0 to 20 N were applied to the indenter as it was automatically drawn across the sample surface at a rate of 0.27 mm/s. The micrograph of scratches trace was observed by scanning electron microscope (JEM-1200EX, operating voltage 40 kV, and deposited Au film).

The ion-induced interfacial mixing was examined using scanning Auger electron spectroscopy (AES). AES analyses were obtained from a Perkin-Elmer PHI 595 scanning Auger microprobe. The base pressure in the PHI 595 AES system was about 4×10^{-6} Pa. The four elements (C, N, O, Ag) Auger transitions were selected for depth profile analysis. Sputter depth profiling was performed by 3.0 kV Ar^+ ion beam over a $0.3 \times 0.3 \text{ mm}^2$ area, the incident Ar^+ ion beam was at 45 angle to the sample surface. The layer phase of mixing on implanted sample was performed on the X-ray diffractometer of D/Max-RB which was operated at 50 kV and 100–150 mA with $\text{CuK}\alpha$ radiation filtered by a curved graphite crystal monochromator with a special method called sample tilting (STD) reported [13],

in which the azimuthal angle was defined as the angle made by the film surface and the observed lattice planes. This method is very useful for determining structures of the solid films [14]. The atomic concentration of implanted Al_2O_3 surface was obtained by X-ray photoelectron spectroscopy (PHI-550, excited $\text{MgK}\alpha$). In order to reach the desired depth for analysis, an etching method with a 3 kV Ar ion gun was used under the pressure of 1×10^{-6} Pa for 30 s.

In order to test this experiments were performed with smooth spheres of relatively large radius at low loads so that no visible deformation was produced on either the sphere or the polished flat. The frictional coefficient of samples in air was determined by Drive friction precise measuring apparatus (DFPM), for which the block implanted sample is reciprocated against a stationary $\Phi 3$ mm ball (AISI-C-52100, Vickers hardness $H_v = 740$, surface roughness $0.02 \mu\text{m}$), load 2 N, linear velocity 2 mm/s, each sliding distances 10 mm. The tangential frictional force was measured with an instrumented arm and recorded on a chart recorder. Coefficient of sliding friction, μ were determined by taking the value of friction force along the track and dividing by the normal load. In this case, the friction force is expected to be dominated by contact adhesion [1].

3. Results and discussion

3.1. Adhesion

The adhesion of the ion-plating Ag and ion implanted Ag films on Al_2O_3 (104) was evaluated using a scratch test. The minimum force required to remove a film and fracture a substrate from a scratch were used as a measure of adhesion and substrate toughness. The results from these scratch tests are summarized in Table I. Scanning electron micrographs showing film removal from the ion-plating Ag specimen and from those Ag/ Al_2O_3 specimen implanted with $1 \times 10^{17} \text{ N}^+ \cdot \text{cm}^{-2}$ are presented in Fig. 1.

The Ag film was removed from the ion-plating specimen about 4 N, which was the minimum force that

TABLE I Critical peeling load of N^+ implanted on Ag/ Al_2O_3

| Sample | Ag/ Al_2O_3 | Implanting dose (ions $\cdot \text{cm}^{-2}$) | | |
|---------------------------|-----------------------------|--|--------------------|--------------------|
| | | 1×10^{15} | 1×10^{16} | 1×10^{17} |
| Critical peeling load (N) | 4.0 | 11.0 | 12.0 | 13.3 |



Figure 1 Scratch photograph of Ag/ Al_2O_3 samples (a) Unimplanted and (b) $1 \times 10^{17} \text{ N}^+ \cdot \text{cm}^{-2}$.

could be applied. As shown Fig. 1a, the Ag film was completely removed from the scratch without any sign of Ag deformation or smearing. The debris produced from the unimplanted material was sharp and angular and thus had its origins in brittle fracture around the scratch. The groove in the unimplanted region is accompanied by cracks that extend into the surrounding material for distances comparable to the groove width. This suggests that the film was removed by brittle interfacial failure as a result of stress build-up at a discrete interface [15, 16] (Fig. 1a). Ag film on Al₂O₃ substrate showed poor bond strength and were delaminated from the beginning stage. An adhesion modification as a function of irradiation fluence by means of the scratch test is in progress and will be reported separately together with the results of adhesion changes on the Ag-coated samples as a function of ion irradiation fluence. After implanting a dose of 1×10^{15} N/cm², the critical force increased greatly to 11 N. The critical force was further increased slowly to 13.3 N at 1×10^{17} N · cm⁻² dose. The film implanted with high doses were not removed as a result of brittle interfacial failure, but were removed as a result of catastrophic substrate failure. As shown in (Fig.1b) for a specimen implanted with 1×10^{17} N · cm⁻², film deformation and smearing accompanied the removal of these films. Film removal did not occur at a single abrupt interface, but occurred in a mixed mode throughout the scratch trace. The debris produced from the high-dose implanted material is more round indicating its origin in plastic deformation. It is immediately obvious that the amount of lateral cracking and the resultant sappling of material was much less in the implanted region. The implanted surface prevents subsurface cracks from reaching the free surface. The effect of amorphization can be neglect in this work, because the amorphous of Al₂O₃ layer formed when N implantation dose was above 1×10^{17} N · cm⁻² [17]. Ag films on Al₂O₃ were chosen as a model system for studying the adhesion between metal films and ceramic. These results of the scratch test indicate that the bond strength between Ag plating film and Al₂O₃ substrate was significantly increased by the N implantation.

3.2. Ion-induced interfacial mixing

Both the range and the damage distributions beneath the surface may be approximated to gaussian profiles. The 0.11 ± 0.02 μm thickness of the ion-plating Ag film was chosen to match the calculated mean projected range 0.11 μm of 110 keV N⁺ by the Monte Carlo method TRIM88 (Table II). It has been shown that electronic energy losses $(dE/dX)_e$ was more than nuclear energy losses $(dE/dX)_n$, the electronic energy losses and nuclear energy losses near the interface, thus may project the interface of ion-plating Ag/substrate and key roles for improving adhesion.

TABLE II Range for the material implanted

| Energy loss (keV · μm ⁻¹) | | Projected mean ion range R_p (μm) | Standard derivation ΔR_p (μm) |
|---------------------------------------|-------------|--|--|
| $(dE/dX)_e$ | $(dE/dX)_n$ | | |
| 501.4 | 113.5 | 0.11 | 0.07 |

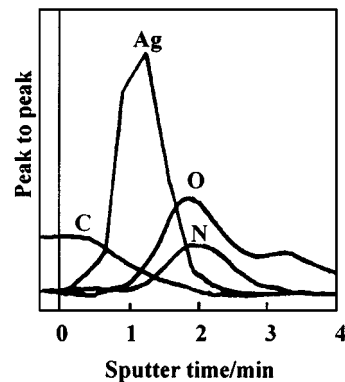


Figure 2 The AES depth profiling of implanted Ag/Al₂O₃ at 1×10^{17} N · cm⁻² dose.

In order to determine the amount of Ag mixed after ion bombardment. The depth profiling and layer phase of the N⁺ implanted (1×10^{17} cm⁻²) Ag/Al₂O₃ specimen was examined using AES and STD analysis in conjunction with scratch test. AES analyses (Fig. 2) performed in the regions of the sputter time exhibited a mixture of Ag, O and N. Ag atom was maximum concentration about 1 min sputter time, but N and O in 2 min, N penetrated the whole Ag film and reached Al₂O₃. There appear to be Ag/Al₂O₃ interacting with both the Ag films and the Al₂O₃ substrates.

The integrity of the Ag film has been altered by the incorporation of O, N intermediate layer and ion mixing process. The interface between the Ag and the Al₂O₃ has been graded slightly [12]. The interfacial grading increased interfacial integrity and adhesion by distributing applied stress over a larger interfacial volume. In addition, the graded distribution of Ag-N and Ag-O produced by the implantation suggests the formation of adhesive bonding across the interfaces [18, 19]. The objective here was to determine the chemical interactions in the Ag-rich and O-rich regions of the Ag/Al₂O₃ interface, and they were influenced by the N⁺ implantation. As shown in Fig. 3 for sputter 8 min specimens, this Al/O ratio was extremely close to the value (2/3) expected for Al₂O₃ and appear N. The interface between

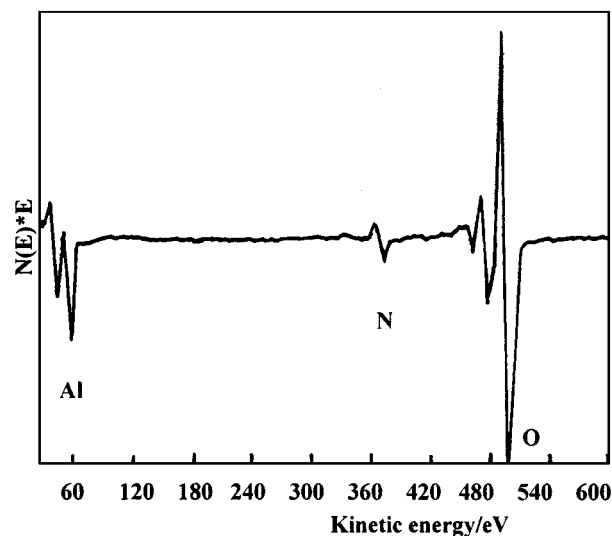


Figure 3 The AES spectra after sputter 8 min on implanted Ag/Al₂O₃ of 1×10^{17} N · cm⁻² dose.

TABLE III Atomic concentration (%) after sputter 30 s on implanted Ag/Al₂O₃

| | Al | N | Ag | O | C |
|---|-----|-----|------|------|------|
| $1 \times 10^{15} \text{ N} \cdot \text{cm}^{-2}$ | 2.3 | 3.5 | 37.2 | 5.8 | 51.2 |
| $1 \times 10^{17} \text{ N} \cdot \text{cm}^{-2}$ | 3.1 | 4.3 | 22.6 | 22.9 | 47.2 |

the Ag and the Al₂O₃ was rather abrupt in the as-plating specimens. The N has been dispersed primarily into the Ag film, but also into the Al₂O₃ substrate. Atomic concentration of XPS spectra obtained from this specimen are shown in Table III. The surfaces of the implanted specimens after sputter 30 s, Al, N, O concentrations increased and Ag decreased with increasing dose, thus recoiled Al and mixed Ag obviously appeared.

Thus the additional adhesion increase observed for N⁺ implantation with a intermediate layer must be attributed to the interfacial grading and the chemical bonding across the interface produced by these methods. The chemistry of the N was of particular importance since the interfacial Ag and Al₂O₃ have been observed to chemically interact under similar ion-induced mixing. The extent of interfacial mixing, interfacial grading and Ag dispersion increased slightly as the implantation dose. The interfacial mixing observed in these ion implanted Ag/Al₂O₃ specimens did not occur through simple diffusion. The main aspect revealed by this study was the creation by the ion beam of new chemical bonding at the interface between atoms of the metal film and the Al₂O₃ substrate, but this reaction was formation of any continuous interfacial layer. Spectra in order to support our designating, and a mixed interface that can enhance the adhesion strength, therefore, we suggest that the interlayer compounds between Ag and Al₂O₃ give rise to the enhanced interfacial adhesion strength. X-ray diffraction experiments (STD) on the specimens (implanted $1 \times 10^{17} \text{ N} \cdot \text{cm}^{-2}$) revealed that a metal ceramic of compound $13\text{Al}_2\text{O}_3 \cdot \text{AlN}$ [20] and $\alpha\text{-AgAlO}_2$ [21] was formed (Fig. 4). The surface layer of the specimen was thought to be a mixed phase of $13\text{Al}_2\text{O}_3 \cdot \text{AlN}$ and $\alpha\text{-AgAlO}_2$. This was in contrast to the result for N implantation and was thought to be related to the new compound formation with non equilibrium processes of implantation. Perhaps, the generation of metal ceramic compounds in implantation layer

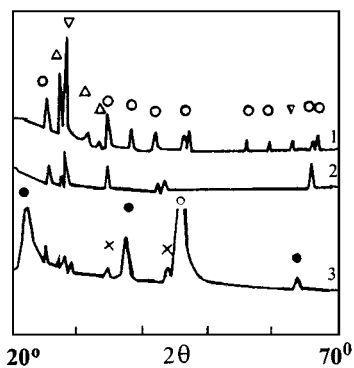


Figure 4 The STD patterns of the samples: (1) ruby, (2) implanted Al₂O₃ at $1 \times 10^{17} \text{ N} \cdot \text{cm}^{-2}$ dose, (3) implanted Ag/Al₂O₃ at $1 \times 10^{17} \text{ N} \cdot \text{cm}^{-2}$ dose. ○: $\alpha\text{-Al}_2\text{O}_3$, Δ: $\epsilon\text{-Al}_2\text{O}_3$, ▽: CrO₃, ●: $13\text{Al}_2\text{O}_3 \cdot \text{AlN}$ and ×: $\alpha\text{-AgAlO}_2$.

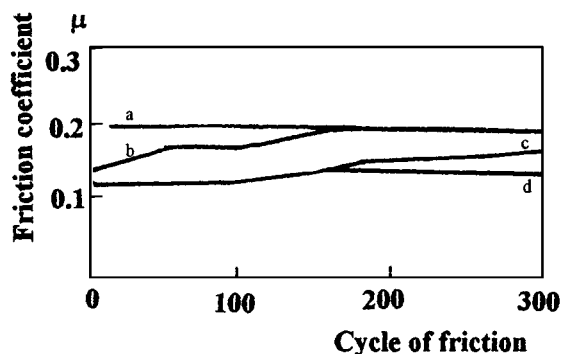


Figure 5 Friction coefficient of Ag/Al₂O₃ for sliding cycles (a) unimplanted (b) $1 \times 10^{15} \text{ N} \cdot \text{cm}^{-2}$ (c) $1 \times 10^{16} \text{ N} \cdot \text{cm}^{-2}$ (d) $1 \times 10^{17} \text{ N} \cdot \text{cm}^{-2}$.

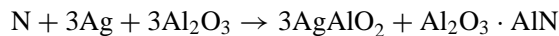
also affected the crack propagation process and caused the increase of the fracture toughness.

After implanting with $1 \times 10^{17} \text{ N} \cdot \text{cm}^{-2}$, a substantial quantity of carbon has been mixed into the Ag films with most of it segregating to the surface (Fig. 2, Table III). The layer contained carbon that was incorporated with the implantation process in lower vacuum. Tribology concerns the interactions between surfaces in contact while moving with respect to one another and includes phenomena such as friction. Fig. 5 shows graphs of friction coefficient against cycle on samples. The coefficient show a constant value in the 300 cycles of travel on unimplanted sample, was about 0.2 due to the friction between ball and soft Ag film. From the implanted samples it can be seen that the friction force gradually increases with sliding distance. Another feature of the friction in implanted samples was that the highest dose specimens showed a decrease in friction. At $1 \times 10^{15} \text{ cm}^{-2}$ dose, the friction after 150 cycles increased up to a maximum at the onset of the ion-plating Ag film, which was equal to friction between Ag and metal. As interfacial bond increased and the shear strength of contact region decreased at high dose may result in the decrease of adhesive friction and such a change in frictional mechanism could affect the use of ion-mixing [1]. Friction decreased in initial cycle where ion implantation doses lead to surface carbon film. This was an indication that the adhesion between the steel and the implanted surface had changed, the carbon film may interfere with the slider/substrate adhesion and produce changes in the adhesion component of friction. When the thin carbon film broken at which the ion mixing layer reaches the surface contact, the friction has increased. As the thickness of such surface carbon film is increased with increasing dose, the lubrication effects will become more important and reduce to their adhesion between the ball and implanted plat, it will be the major effects likely to contribute to the initial measured lower friction.

3.3. Interfacial reaction

A last comment concerns the validity of the “enthalpy rule” when applied to the Ag/Al₂O₃ system. This semi-empirical rule only gives a qualitative indication about the mixing at metal/ceramic interfaces. In general, mixing occurs if ΔH , is negative for at least one possible

chemical reaction between the metal and the Al₂O₃ substrate, but the some chemical reaction is not according to semi-empirical “enthalpy rule” in non equilibrium processes of implantation. According to above, we explain that the reaction of Ag with Al₂O₃ should produce the following:



This is the case for the Ag/Al₂O₃ reaction leading to metal ceramic of 13Al₂O₃ · AlN and α-AgAlO₂ formation though non equilibrium processes. In addition, the N⁺ implantation produced new chemical bonding at the Ag/Al₂O₃ interfaces. This is evident in the scratch tests showed the presence of Ag/Al₂O₃ bonding in the interface of the films. This investigation resulted in extensive interfacial grading, and new chemical bonding across the Ag/Al₂O₃ interfaces. The combination of these effects provided an adhesion increase that was approximately 3 times that obtained in unimplanted Ag/Al₂O₃ specimens.

4. Conclusions

After ion beam mixing, the adhesion strength of Ag/Al₂O₃ increases dramatically, the adhesive bond of Ag films on Al₂O₃ could be enhanced greatly by N⁺ implantation through the interface at a specimen. The adhesion increase was attributed to the ion mixing. This study was the creation by the ion beam of new chemical bonding at the interface between atoms of the Ag film and the Al₂O₃ substrate. The case for the Ag/Al₂O₃ reaction lead to 13Al₂O₃ · AlN and α-AgAlO₂ formation though non equilibrium processes, and friction decreased in initial cycle where ion implantation of lower vacuum lead to surface carbon film. The combination of these effects provided an adhesion increase that was

approximately 3 times that obtained in unimplanted Ag/Al₂O₃ specimens.

References

1. S. J. BULL and T. F. PAGE, *J. Mater. Sci.* **30** (1995) 5356.
2. T. HIOKI, A. ITOH, S. NODA, H. DOI, J. KAWAMOTO and O. KAMIGAITO, *Nucl. Instrum. Methods* **B7/8** (1985) 521.
3. F. HALITIM, N. IKHLEF, B. L. BOUDOUKHA and G. FANTOZZI, *J. Phys. D.* **30** (1997) 330.
4. P. J. BURNETT and T. F. PAGE, *Wear.* **114** (1987) 85.
5. D. K. SOOD and J. E. E. BAGLIN, *Nucl. Instrum. Methods* **B19/20** (1987) 954.
6. G. S. CHANG, S. M. JUNG, Y. S. LEE, I. S. CHOI, C. N. WHANG, J. J. WOO and Y. P. LEE, *J. Appl. Phys.* **81** (1997) 135.
7. G. B. KREFFT and E. P. EERNISSE, *ibid.* **49** (1978) 2725.
8. C. J. MCHARGUE, *Nucl. Instrum. Methods* **B19/20** (1987) 797.
9. A. A. GALUSKA, *J. Vacuum Sci. Technol.* **B5** (1987) 1.
10. J. E. E. BAGLIN and G. J. CLARK, *Nucl. Instrum. Methods* **B7/8** (1985) 881.
11. C. J. MCHARGUE, in “Structure-Property Relationships in Surface Modified Ceramics,” edited by C. J. McHargue, R. Kossowsky and W. O. Hofer (Kluwer, Dordrecht, 1989) pp.117.
12. L. ROMANA, P. THEVENARD, R. BRENIER, G. FUCHS and G. MASSOURAS, *Nucl. Instrum. Methods* **B32** (1988) 96.
13. Q. Z. CONG, D. Y. YU and L. J. WENG, *Thin Solid Films* **213** (1992) 13.
14. Q. Z. CONG, D. Y. YU, J. WANG and Y. J. OU, *ibid.* **209** (1992) 1.
15. A. A. GALUSKA, J. C. UHT and P. M. ADAMS, *J. Vacuum Sci. Technol.* **A6** (1988) 99.
16. A. A. GALUSKA, J. C. UHT and N. MARQUEZ, *ibid.* **A6** (1988) 110.
17. Q. Z. WANG, Y. F. CHEN, J. TIAN, X. H. YANG and Z. H. WANG, *Nuclear Techniques (in Chinese)* **19** (1996) 75.
18. A. A. GALUSKA, *Appl. Surface Sci.* **40** (1989) 33.
19. *Idem.*, *ibid.* **40** (1989) 19.
20. Powder Diffraction File Card, 26-33.
21. Powder Diffraction File Card, 21-1069.

Received 26 October 1997

and accepted 30 November 1998